MorphGrower: A Synchronized Layer-by-layer Growing Approach for Plausible Neuronal Morphology Generation

Nianzu Yang, Kaipeng Zeng, Haotian Lu, Yexin Wu, Zexin Yuan, Danni Chen, Shengdian Jiang, Jiaxiang Wu, Yimin Wang, Junchi Yan

Presenter: Nianzu Yang

2024-07-23

ICML

International Conference On Machine Learning

Background

Neuroscience

Neuroscience provides insights into cognitive processes and neural mechanisms, inspiring AI algorithms.

A Virtuous Cycle

AI aids in analyzing complex neural data and simulating brain functions, enhancing neuroscience research.

AI

Background

Why morphology data are important?

- The morphology determines which spatial domain can be reached for a certain neuron, governing the connectivity of the neuronal circuits [1]
- Neuronal morphology also defines how a neuron integrates the signal inputs received from other neurons to produce outputs [2]
- Studying neuronal morphologies also facilitates the discovery of therapies for brain disorders and some degenerative diseases, e.g. mental retardation [3], autism[4] and Alzheimer [5]

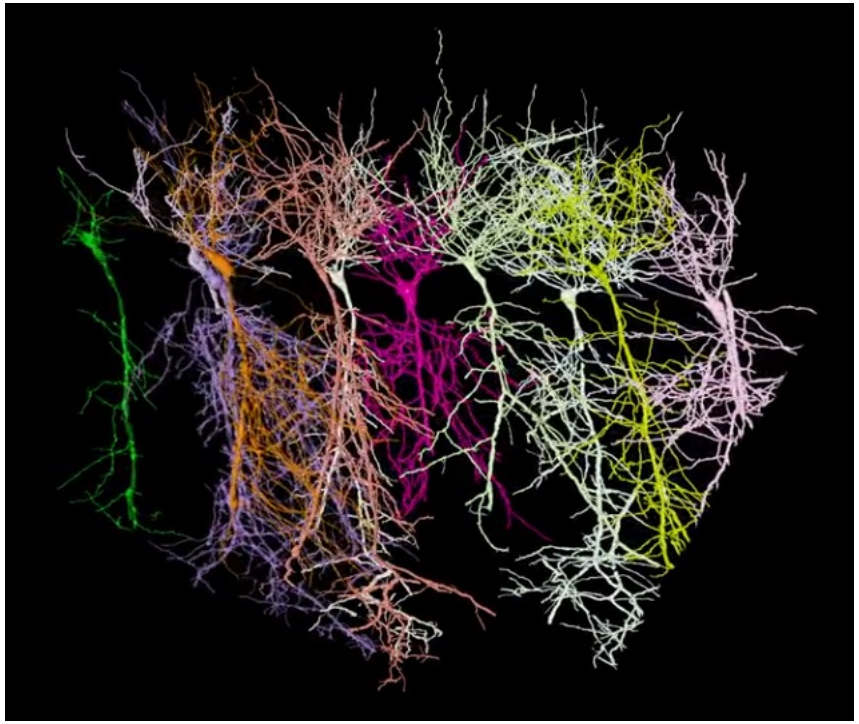

Background

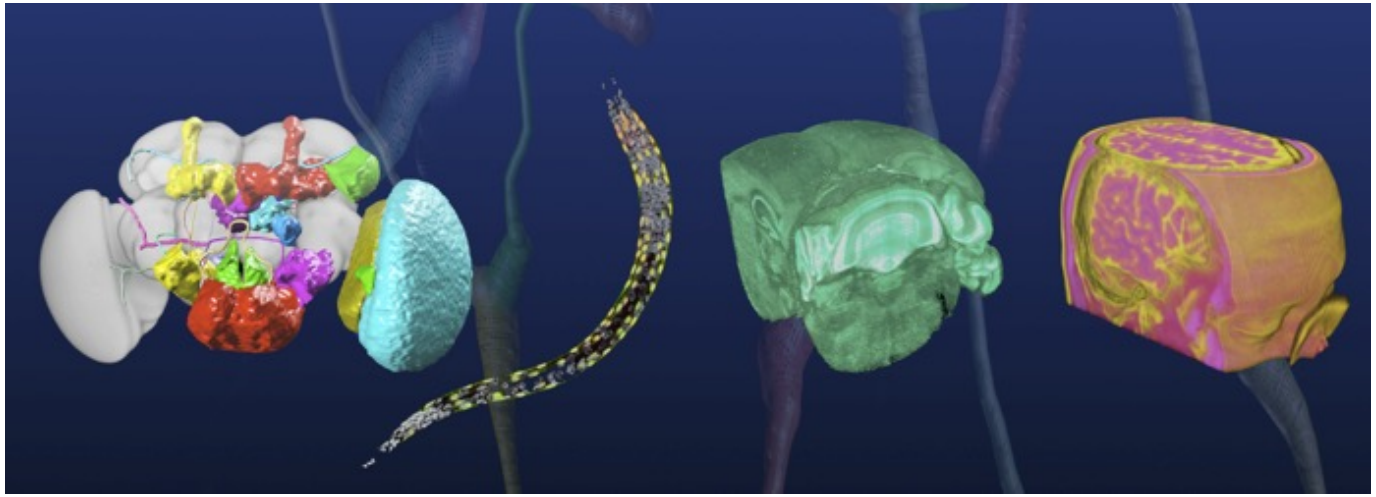

- A worm's brain: 302 neurons
- A fly's brain: 100,000 neurons
- A mouse's brain: 10^7~10^8 neurons
- A human being's brain: 10^{11} neurons

The traditional way to collect quality neuronal morphologies involves three key steps: *i)* histological preparation, *ii)* microscopic visualization and *iii)* accurate tracing.

labor-intensive | time-consuming | potentially subject to human bias and error

We can opt to generate plausible morphology samples by computational approaches.

Baseline: MorphVAE [6]
the only existing learning-based method

Preliminaries

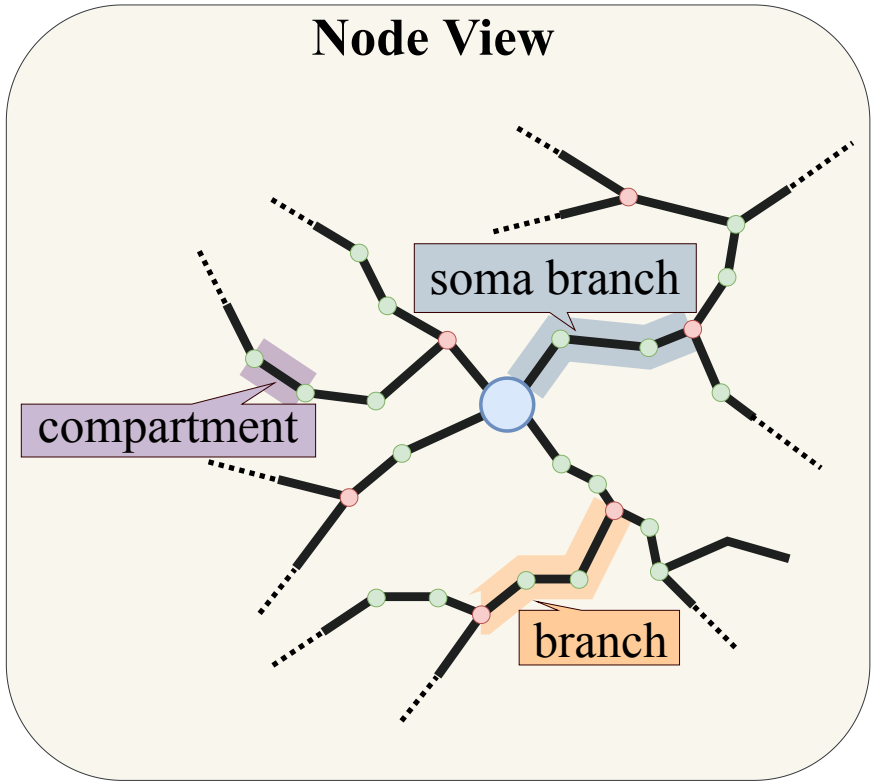

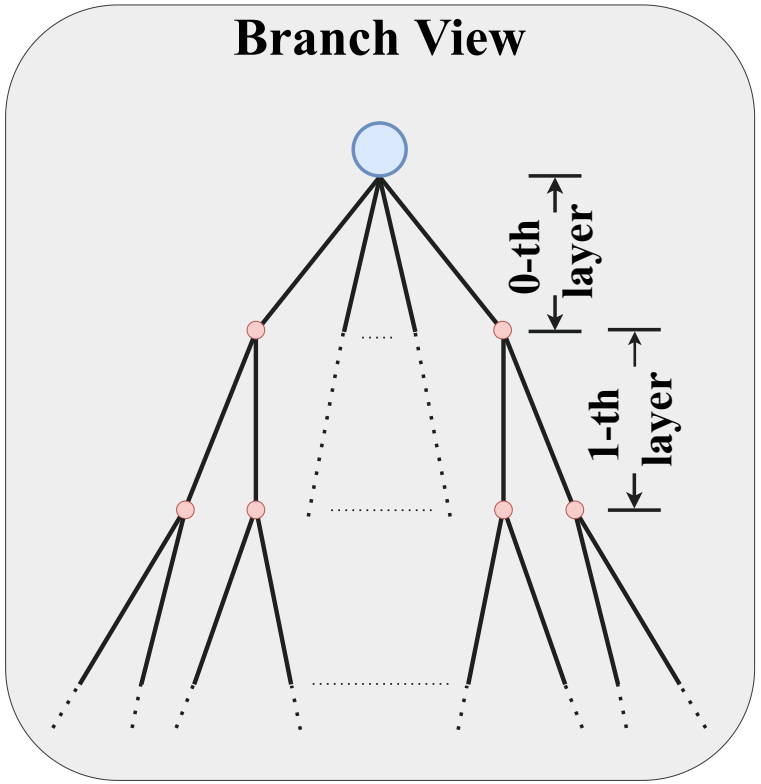

A neuronal morphology is described as a set of nodes in three-dimensional space, with each node associated with a coordinate in this space.

Neuronal morphology is a tree-like structure.

Key Concepts:

- **Soma:**
  the root node (unique)
  can have ≥ 2 outgoing edges
- **Tips:**
  the leaf nodes
- **Bifurcations:**
  can only have 2 outgoing edges
- **Branches:**
  the paths starting from a multifurcation (soma or bifurcation) and ending at a bifurcation or a tip

Brief Introduction to MorphVAE

The basic building block of MorphVAE: 3D-walk → the path from the soma to a tip

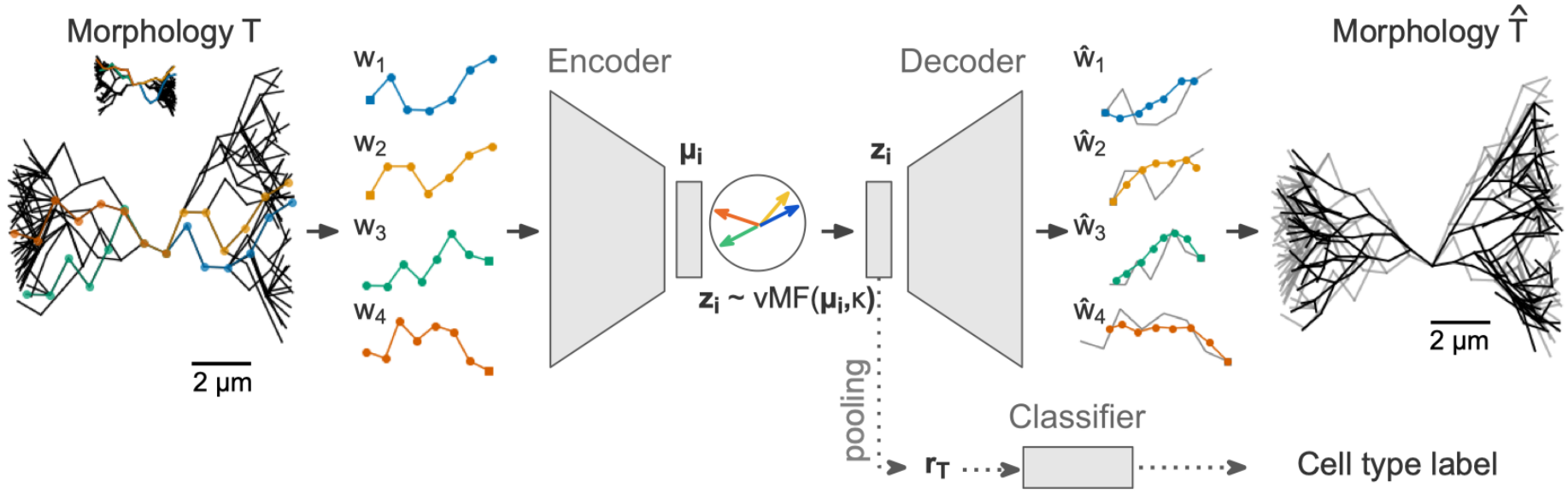

Two steps:

- **generate all 3D-walks in one shot**
- **adopt a post-hoc clustering method on the generated 3D-walks to aggregate some nodes of different 3D-walks**

→ **there may exist other nodes that have > 2 outgoing edges in the final generated morphology besides the soma**

This contradicts a commonly accepted notion that only the soma node can have more than two child branches!

Methodology

Layer-by-layer Generation Strategy

In practice, dendrites or axons grow from soma progressively and may diverge several times in the growing process.

Our strategy mimics the natural growth pattern of neurons to some extent.

MorphVAE violates this!

Following such a layer-by-layer strategy, a new morphology can be obtained by generating new layers and merging them to intermediate generated morphology regressively.

Methodology

Generating Branches in Pairs

As pointed out in previous works [7, 8, 9],

there exists a complex dependency between sibling branches.

If we separate sibling branches from each other and generate each of them individually, this dependency will be hard to model. → **MorphVAE fails in this regard**

A natural idea comes to our mind!

We can regard sibling branches as a whole and generate sibling branches in pairs each time, to implicitly model their internal dependency

Methodology

Conditional Generation

A Key Observation: **grown branches could influence their subsequent branches**

Condition

We propose to encode the intermediate morphology which has been generated into an embedding and restrict the generation of branch pairs in the following layer to be conditioned on this embedding we obtain.

We further split the condition into **local condition** and **global condition**.

Assuming that we are generating one certain pair of branches, we define:

the path from soma to the bifurcation from which the pair to be generated starts → **local condition**

its previous layers structure → **global condition**

Methodology

Conditional Generation (Cont.)

Justifications for the Conditions from a Neuroscience Perspective:

Local: Previous studies [10, 11] show that the dendrites or axons usually extend away from the soma without making any sharp change of direction, thus reflecting that the orientation of a pair of sibling branches is mainly determined by the overall orientation of the path from the soma to the start point of the siblings.

Global: Dendrites/axons establish territory coverage by following the organizing principle of self-avoidance [12, 13, 14]. Self-avoidance refers to dendrites/axons that should avoid crossing, thus spreading evenly over a territory [15]. Since the global condition can be regarded as a set of the local conditions and each local condition can roughly decide the orientation of a corresponding pair of branches, the global condition helps us better organize the branches in the same layer and achieve an even spread.

Methodology

The Distinction of the Soma Branch Layer

There is no proper definition of conditions for the soma branch layer.

The soma branch layer cannot be unified to the conditional generation formulation.

Two approaches

A straightforward solution is to directly present the soma branches as conditional input to the model, which are fairly small in number compared to all the branches → **MorphGrower**

Another slightly more complex approach is to generate the soma branch layer using another VAE without conditions → **MorphGrower†**

Methodology

Overview of MorphGrower

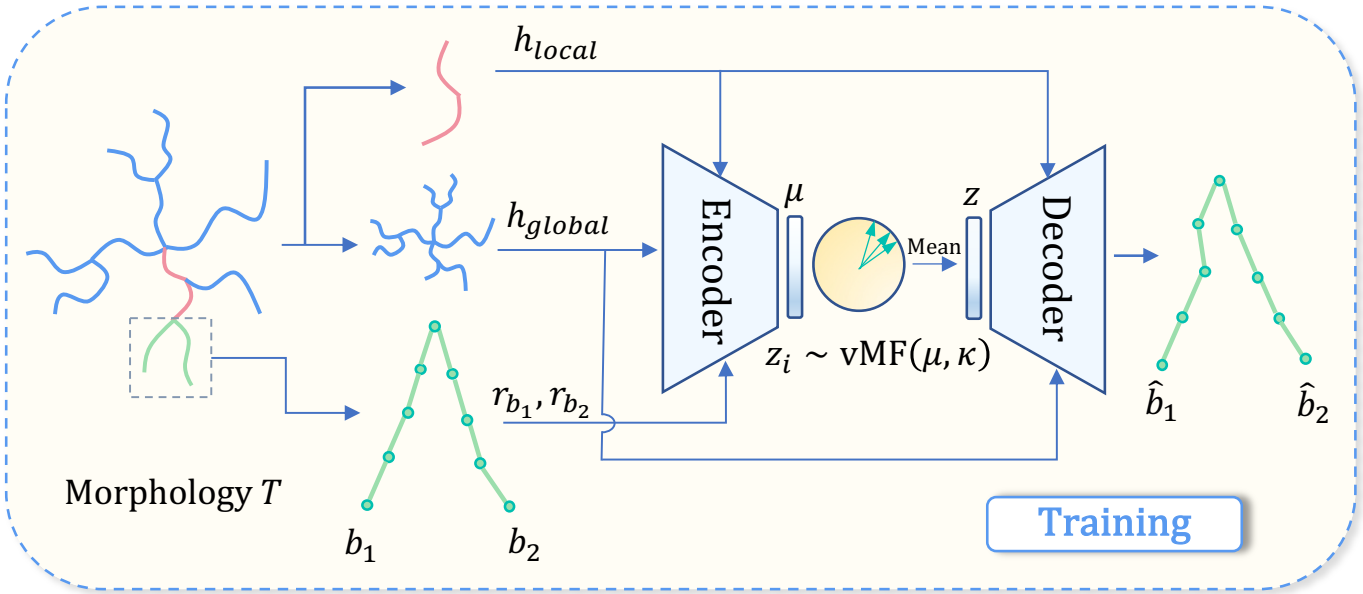

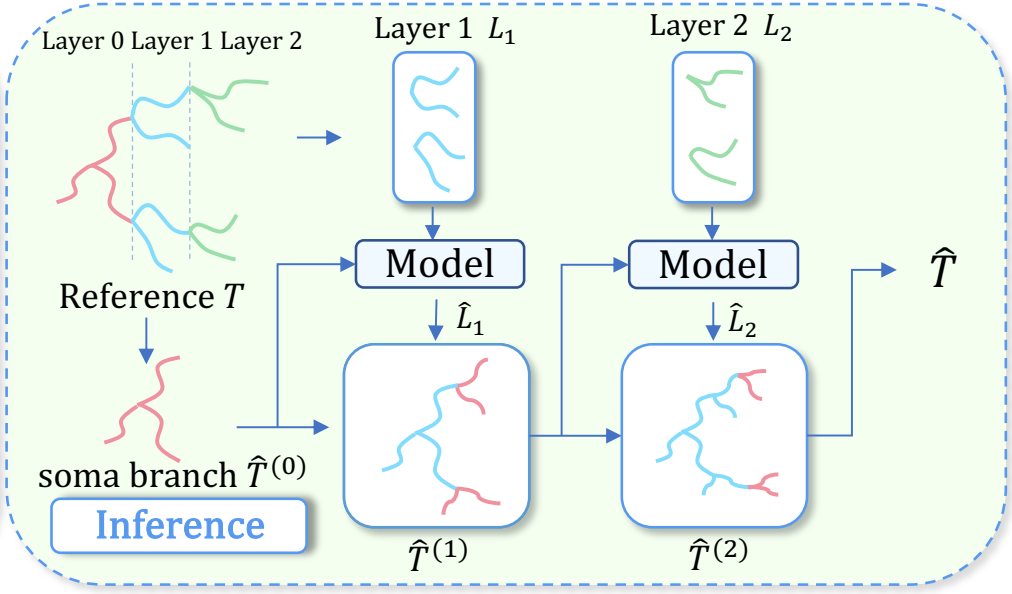

For details on the methods and model instantiation, feel free to scan the two QR codes on the right!

👉

Paper

Code

Experiments

Quantitative Results on Morphological Statistics

Table 1: Performance on the four datasets by the six quantitative metrics. We leave MorphVAE's numbers on MBPL and MAPS blank because it may generate nodes with more than two subsequent branches that conflict with the definition of MBPL and MAPS for bifurcations. **MorphGrower** denotes the version where soma branches are directly provided. Meanwhile, **MorphGrower**† generates soma branches using another unconditional VAE. *Reference* corresponds to the statistical indicators derived from the realistic samples. A closer alignment with *Reference* indicates better performance. The best and the runner-up results are highlighted in **bold** and underline respectively.

Dataset	Method	MBPL / μm	MMED / μm	MMPD / μm	MCTT / %	MASB / °	MAPS / °
VPM	*Reference*	51.33 ± 0.59	162.99 ± 2.25	189.46 ± 3.81	0.936 ± 0.001	65.35 ± 0.55	36.04 ± 0.38
	MorphVAE	41.87 ± 0.66	126.73 ± 2.54	132.50 ± 2.61	0.987 ± 0.001	——	——
	MorphGrower	**48.29 ± 0.34**	**161.65 ± 1.68**	**180.53 ± 2.70**	0.920 ± 0.004	72.71 ± 1.50	**43.80 ± 0.98**
	MorphGrower†	46.86 ± 0.57	159.62 ± 3.19	179.44 ± 5.23	**0.929 ± 0.006**	**59.15 ± 3.25**	46.59 ± 3.24
RGC	*Reference*	26.52 ± 0.75	308.85 ± 8.12	404.73 ± 12.05	0.937 ± 0.003	84.08 ± 0.28	50.60 ± 0.13
	MorphVAE	43.23 ± 1.06	248.62 ± 9.05	269.92 ± 10.25	0.984 ± 0.004	——	——
	MorphGrower	**25.15 ± 0.71**	**306.83 ± 7.76**	**384.34 ± 11.85**	**0.945 ± 0.003**	**82.68 ± 0.53**	**51.33 ± 0.31**
	MorphGrower†	23.32 ± 0.52	287.09 ± 5.88	358.31 ± 8.54	0.926 ± 0.004	76.27 ± 0.86	49.67 ± 0.41
M1-EXC	*Reference*	62.74 ± 1.73	414.39 ± 6.16	497.43 ± 12.42	0.891 ± 0.004	76.34 ± 0.63	46.74 ± 0.85
	MorphVAE	52.13 ± 1.30	195.49 ± 9.91	220.72 ± 12.96	0.955 ± 0.005	——	——
	MorphGrower	**58.16 ± 1.26**	**413.78 ± 14.73**	**473.25 ± 19.37**	0.922 ± 0.002	**73.12 ± 2.17**	**48.16 ± 1.00**
	MorphGrower†	54.63 ± 1.07	398.85 ± 18.84	463.24 ± 22.61	**0.908 ± 0.003**	63.54 ± 2.02	48.77 ± 0.87
M1-INH	*Reference*	45.03 ± 1.04	396.73 ± 15.89	705.28 ± 34.02	0.877 ± 0.002	84.40 ± 0.68	55.23 ± 0.78
	MorphVAE	50.79 ± 1.77	244.49 ± 15.62	306.99 ± 23.19	0.965 ± 0.002	——	——
	MorphGrower	**41.50 ± 1.02**	**389.06 ± 13.54**	**659.38 ± 30.05**	0.898 ± 0.002	**82.43 ± 1.41**	61.44 ± 4.23
	MorphGrower†	37.72 ± 0.96	349.66 ± 11.40	617.89 ± 27.87	**0.876 ± 0.002**	78.66 ± 1.12	**57.87 ± 0.96**

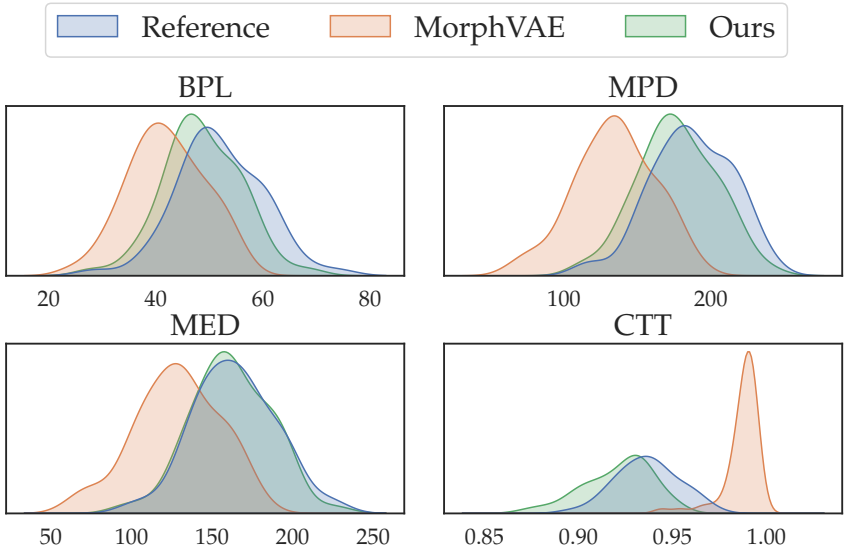

MorphGrower significantly outperforms MorphVAE!

Experiments

Generation Plausibility with Real/Fake Classifier

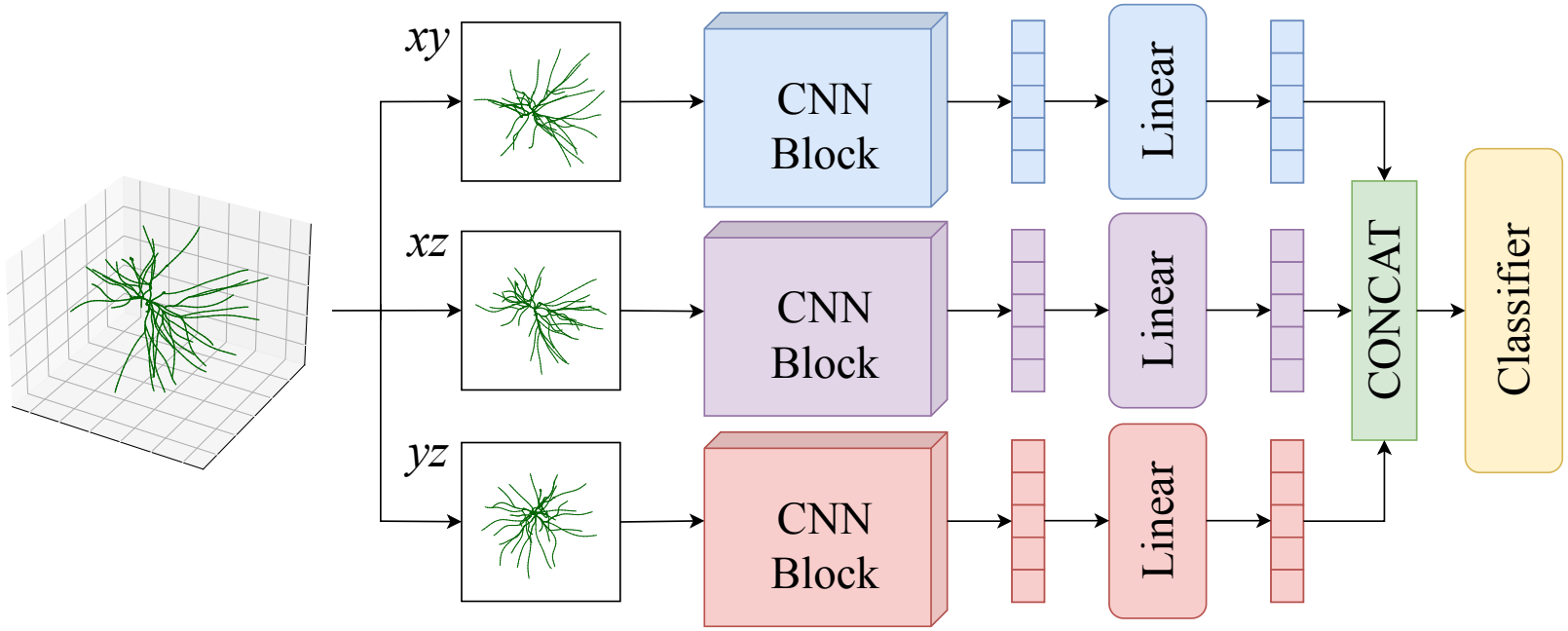

Table 2: Classification accuracy (%). Accuracy approaching 50% indicates higher plausibility.

Method \ Dataset	VPM	RGC	M1-EXC	M1-INH
MorphVAE	86.75 ± 06.87	94.60 ± 01.02	80.72 ± 10.58	91.76 ± 12.14
MorphGrower	54.73 ± 03.36	62.70 ± 05.24	55.00 ± 02.54	54.74 ± 01.63

we have presented our generated samples to neuroscience domain experts and receive positive feedback for their realistic looking

harder to be distinguished from real samples

Experiments

The Electrophysiological Response Simulation Results

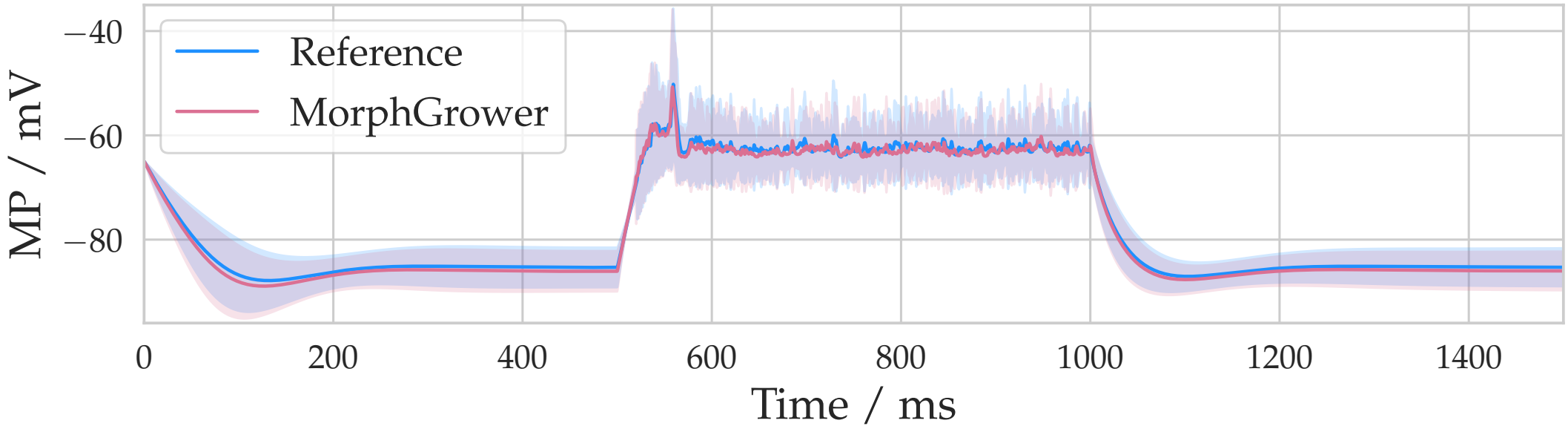

Table 3: Simulated recording statistical characteristics.

Metric	MMF / Hz	MMAPH / mV	MMAHPD / mV	MMAPA / mV
Reference	9.328	43.021	25.666	-77.231
MorphGrower	9.384	44.382	26.606	-77.837
Relative Error	0.60%	3.17%	3.66%	0.78%

The electrophysiological responses of real and our generated samples exhibit a high degree of similarity.

Experiments

Ablation study

Table 10: The result of ablation study on the four datasets by six quantitative metrics. The best and the runner-up in each columns are highlighted in **bold** and underline respectively. We leave MorphVAE's numbers on MBPL and MAPS blank because it may generate nodes with more than two subsequent branches that conflict with the definition of MBPL and MAPS for bifurcations. A closer alignment with *Reference* indicates better performance.

Dataset	Method	MBPL / μm	MMED / μm	MMPD / μm	MCTT / %	MASB / °	MAPS / °
VPM	*Reference*	51.33 ± 0.59	162.99 ± 2.25	189.46 ± 3.81	0.936 ± 0.001	65.35 ± 0.55	36.04 ± 0.38
	MorphVAE	41.87 ± 0.66	126.73 ± 2.54	132.50 ± 2.61	0.987 ± 0.001	——	——
	MorphGrower	**48.29 ± 0.34**	161.65 ± 1.68	180.53 ± 2.70	0.920 ± 0.004	72.71 ± 1.50	**43.80 ± 0.98**
	LSTM → Transformers	47.40 ± 0.88	**162.46 ± 3.82**	**180.87 ± 3.09**	0.943 ± 0.010	**70.94 ± 2.77**	53.86 ± 0.99
	- Local Condition	40.90 ± 0.79	137.47 ± 2.63	162.53 ± 3.24	0.911 ± 0.006	74.55 ± 0.88	58.22 ± 0.32
	- Global Condition	44.51 ± 0.78	153.84 ± 3.56	173.58 ± 5.41	0.938 ± 0.003	71.29 ± 3.56	47.06 ± 0.59
	- EMA	45.24 ± 0.22	155.11 ± 1.98	173.68 ± 2.86	**0.936 ± 0.005**	67.79 ± 1.45	46.28 ± 0.08
RGC	*Reference*	26.52 ± 0.75	308.85 ± 8.12	404.73 ± 12.05	0.937 ± 0.003	84.08 ± 0.28	50.60 ± 0.13
	MorphVAE	43.23 ± 1.06	248.62 ± 9.05	269.92 ± 10.25	0.984 ± 0.004	——	——
	MorphGrower	**25.15 ± 0.71**	306.83 ± 7.76	384.34 ± 11.85	**0.945 ± 0.003**	82.68 ± 0.53	51.33 ± 0.31
	LSTM → Transformers	25.10 ± 0.65	**308.35 ± 7.34**	**387.67 ± 10.55**	0.948 ± 0.003	**84.04 ± 0.33**	52.35 ± 0.14
	- Local Condition	23.56 ± 0.74	294.01 ± 8.21	363.86 ± 11.36	0.954 ± 0.003	79.67 ± 1.17	54.44 ± 0.36
	- Global Condition	22.99 ± 0.83	293.87 ± 9.01	354.95 ± 11.85	0.954 ± 0.006	78.19 ± 4.10	**50.96 ± 0.63**
	- EMA	23.38 ± 0.66	295.09 ± 8.76	359.76 ± 8.76	0.951 ± 0.005	78.47 ± 1.84	52.25 ± 0.44
M1-EXC	*Reference*	62.74 ± 1.73	414.39 ± 6.16	497.43 ± 12.42	0.891 ± 0.004	76.34 ± 0.63	46.74 ± 0.85
	MorphVAE	52.13 ± 1.30	195.49 ± 9.91	220.72 ± 12.96	0.955 ± 0.005	——	——
	MorphGrower	**58.16 ± 1.26**	**413.78 ± 14.73**	**473.25 ± 19.37**	**0.922 ± 0.002**	73.12 ± 2.17	**48.16 ± 1.00**
	LSTM → Transformers	56.75 ± 1.49	415.90 ± 4.39	472.30 ± 7.99	0.942 ± 0.005	72.97 ± 1.75	51.06 ± 0.98
	- Local Condition	55.85 ± 1.24	409.66 ± 7.36	464.18 ± 9.07	0.940 ± 0.004	**73.81 ± 1.24**	51.54 ± 0.84
	- Global Condition	55.01 ± 0.65	404.42 ± 8.67	453.58 ± 11.90	0.955 ± 0.007	71.72 ± 1.23	48.48 ± 1.04
	- EMA	55.71 ± 1.24	407.29 ± 16.28	458.49 ± 12.29	0.951 ± 0.008	72.61 ± 4.35	50.20 ± 0.83
M1-INH	*Reference*	45.03 ± 1.04	396.73 ± 15.89	705.28 ± 34.02	0.877 ± 0.002	84.40 ± 0.68	55.23 ± 0.78
	MorphVAE	50.79 ± 1.77	244.49 ± 15.62	306.99 ± 23.19	0.965 ± 0.002	——	——
	MorphGrower	**41.50 ± 1.02**	**389.06 ± 13.54**	**659.38 ± 30.05**	**0.898 ± 0.002**	82.43 ± 1.41	61.44 ± 4.23
	LSTM → Transformers	40.55 ± 0.82	378.98 ± 12.21	645.68 ± 28.83	0.903 ± 0.003	**84.32 ± 0.85**	59.89 ± 0.91
	- Local Condition	39.33 ± 1.02	383.21 ± 10.06	641.00 ± 23.99	0.918 ± 0.003	77.30 ± 10.86	60.53 ± 0.75
	- Global Condition	38.12 ± 0.26	372.66 ± 10.30	613.76 ± 33.09	0.929 ± 0.003	78.29 ± 3.19	**57.21 ± 0.48**
	- EMA	38.97 ± 0.82	383.77 ± 14.04	636.61 ± 40.45	0.921 ± 0.004	80.09 ± 3.24	58.77 ± 0.91

Snapshots of the Generation

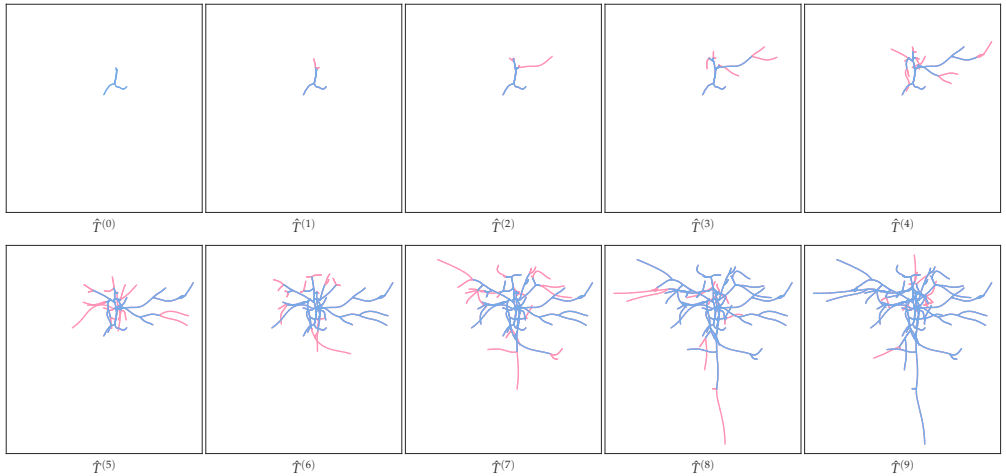

Visualization of Generated Samples

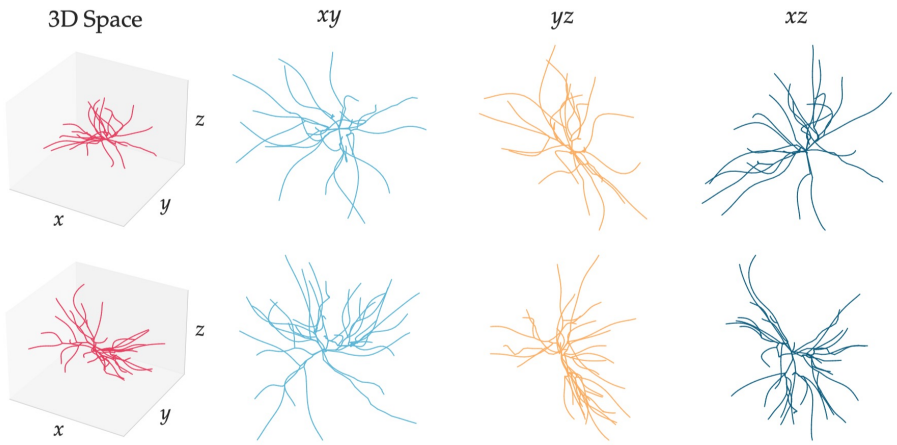

Reference

[1] Memelli, Heraldo, Benjamin Torben-Nielsen, and James Kozloski. "Self-referential forces are sufficient to explain different dendritic morphologies." Frontiers in Neuroinformatics 7 (2013): 1.

[2] Tran-Van-Minh, Alexandra, et al. "Contribution of sublinear and supralinear dendritic integration to neuronal computations." Frontiers in cellular neuroscience 9 (2015): 67.

[3] Dierssen, Mara, and Ger JA Ramakers. "Dendritic pathology in mental retardation: from molecular genetics to neurobiology." Genes, Brain and Behavior 5 (2006): 48-60.

[4] Phillips, Mary, and Lucas Pozzo-Miller. "Dendritic spine dysgenesis in autism related disorders." Neuroscience letters 601 (2015): 30-40.

[5] Lian, Hong, et al. "NFκB-activated astroglial release of complement C3 compromises neuronal morphology and function associated with Alzheimer's disease." Neuron 85.1 (2015): 101-115.

[6] Laturnus, Sophie C., and Philipp Berens. "MorphVAE: Generating Neural Morphologies from 3D-Walks using a Variational Autoencoder with Spherical Latent Space." International Conference on Machine Learning. PMLR, 2021.

[7] Burke, R. E., W. B. Marks, and B. Ulfhake. "A parsimonious description of motoneuron dendritic morphology using computer simulation." Journal of Neuroscience 12.6 (1992): 2403-2416.

[8] Van Pelt, Jaap, Alexander E. Dityatev, and Harry BM Uylings. "Natural variability in the number of dendritic segments: model-based inferences about branching during neurite outgrowth." Journal of Comparative Neurology 387.3 (1997): 325-340.

Reference (Cont.)

[9] Purohit, Prashant K., and Douglas H. Smith. "A model for stretch growth of neurons." Journal of biomechanics 49.16 (2016): 3934-3942.

[10] Samsonovich, Alexei V., and Giorgio A. Ascoli. "Statistical morphological analysis of hippocampal principal neurons indicates cell-specific repulsion of dendrites from their own cell." Journal of neuroscience research 71.2 (2003): 173-187.

[11] López-Cruz, Pedro L., et al. "Models and simulation of 3D neuronal dendritic trees using Bayesian networks." Neuroinformatics 9 (2011): 347-369.

[12] Sweeney, Neal T., Wenjun Li, and Fen-Biao Gao. "Genetic manipulation of single neurons in vivo reveals specific roles of flamingo in neuronal morphogenesis." Developmental biology 247.1 (2002): 76-88.

[13] Sdrulla, Andrei D., and David J. Linden. "Dynamic imaging of cerebellar Purkinje cells reveals a population of filopodia which cross-link dendrites during early postnatal development." The Cerebellum 5 (2006): 105-115.

[14] Matthews, Benjamin J., et al. "Dendrite self-avoidance is controlled by Dscam." Cell 129.3 (2007): 593-604.

[15] Kramer, A. P., and J. Y. Kuwada. "Formation of the receptive fields of leech mechanosensory neurons during embryonic development." Journal of Neuroscience 3.12 (1983): 2474-2486.

Thanks